CHAPTER

9 Speed estimation and sensorless control of alternating current motors

For the position/speed control of a motor, it is necessary for its speed/position information to be used as a feedback signal for the speed/position control loop. As it can be seen in Chapter 5, for the vector control of alternating current (AC) motors, the information on the rotor position is also necessary. To measure the position/speed of the motor, an analog or a digital position sensor is used. Resolver, synchro, and tacho-generator are well known as analog position sensors. A rotary encoder is the most widely used as the digital position sensor.

In this chapter, we will introduce position sensors used in the motor drive systems and examine the speed estimation method from the position sensor signal. Finally, we will introduce the sensorless control methods of AC motors, which do not use position sensors.

9.1 POSITION SENSORS

Besides the position/speed control of a motor, for the vector control of AC motors, a position sensor is needed. In the vector control, a different type of position sensor is used according to the motor used. As discussed in Chapter 5, the absolute position of the rotor (i.e., permanent magnet) is required for the vector control of permanent magnet synchronous motors (PMSMs). Among analog position sensors, a resolver, which can provide information on the absolute position of the rotor, is commonly used for PMSM drives. On the other hand, since the vector control of induction motors does not require the absolute position of the rotor, an incremental encoder is usually used among digital devices.

Now we will explore the resolver and rotary encoder.

9.1.1 RESOLVER

A resolver is a type of rotary electrical transformer connected to the rotating shaft. The resolver produces signals that vary sinusoidally as the shaft rotates. It is commonly used for measuring the absolute position of the rotor. Fig. 9.1

Electric Motor Control. DOI: http://dx.doi.org/10.1016/B978-0-12-812138-2.00009-X

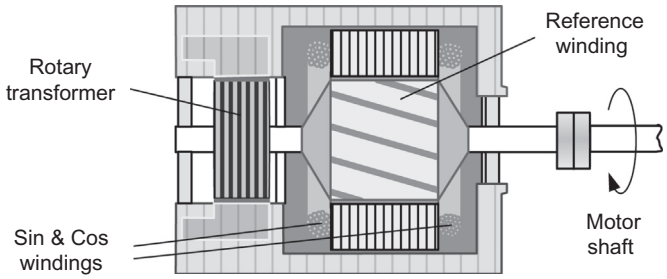

FIGURE 9.1

Resolver.

Source: http://www.amci.com/tutorials/tutorials-what-is-resolver.asp

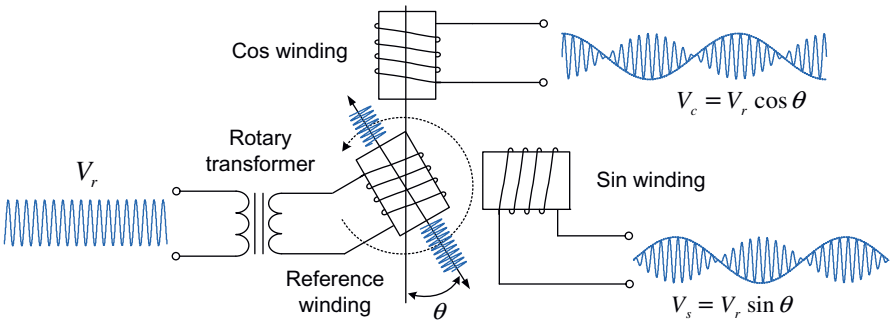

FIGURE 9.2

Resolver windings and their signals.

Source: http://www.amci.com/tutorials/tutorials-what-is-resolver.asp

depicts the configuration of a resolver, which consists of a stator, a rotor, and a rotary transformer [1].

The primary winding of a resolver, called reference winding, is located in the rotor and is excited through a rotary transformer. The two secondary windings, called SIN and COS Windings, are located in the stator and mechanically displaced 90° from each other. In the resolver operation, a shaft angle θ can be measured from signals induced in the secondary windings after injecting AC voltage signal into the primary winding as shown in Fig. 9.2.

When the primary winding is excited by an AC voltage V_r through a rotary transformer, voltages in the secondary windings are induced differently depending on the angle θ of the rotor shaft. The induced voltages vary as sine or cosine of the rotor angle, respectively. From an arctangent function of these signals, we can know the absolute angle θ of the rotor connected to the shaft as

$$\theta = \tan^{-1}\left(\frac{V_c}{V_S}\right) = \tan^{-1}\left(\frac{V_r \sin\theta}{V_r \cos\theta}\right) \tag{9.1}$$

The resolver usually uses a resolver-to-digital converter to provide resolver excitation and convert angular analogue signals of the resolver into a digital form (a serial binary output or pulses equivalent to an incremental encoder) that can be more easily used by digital controllers. The resolver is a rugged device, which can provide a reliable performance in high temperatures, vibration, and contaminated environments. However, resolvers are costly and require complex excitation and signal processing circuits that are susceptible to noise. In practice, a periodical position error may exist due to amplitude imbalance, inductive harmonics, reference phase shift, excitation signal distortion, and disturbance signals [2]. The position error causes a torque ripple with twice the electrical frequency, and thus should be corrected by a compensation method [3].

9.1.2 ROTARY ENCODER

A rotary encoder is a sensor of mechanical motion that generates digital signals in response to the rotational motion of the shaft. There are two main types of rotary encoder according to output forms: the *absolute encoder*, which can provide the absolute value of the rotation angle, and the *incremental encoder*, which provides only the incremental value of the rotation. Incremental encoders are the most widely used for most adjustable motor drive systems because absolute encoders are much more complicated and expensive. There are two sensor types used in encoders to generate digital signals such as magnetic and optical. The latter is more commonly used.

The incremental encoder generates a series of pulses as its shaft moves. These pulses can be used to measure the position, speed, and direction. The resolution of an incremental encoder is frequently described in terms of *pulse per revolution* (PPR), which is the total number of output pulses per complete revolution of the encoder shaft. An encoder with 512 or 1024 PPR is popular in the motor drive systems. The rotary encoders come in two configurations as shown in Fig. 9.3: a *shaft type* that connects the shaft of a rotor with a coupling, and a *hollow type* into which the shaft of a rotor is inserted into.

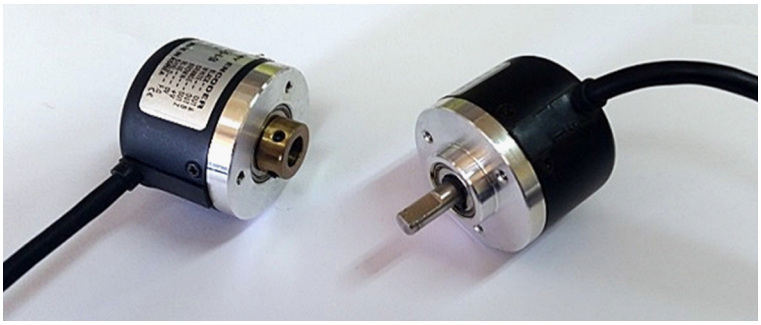

FIGURE 9.3

Incremental encoders.

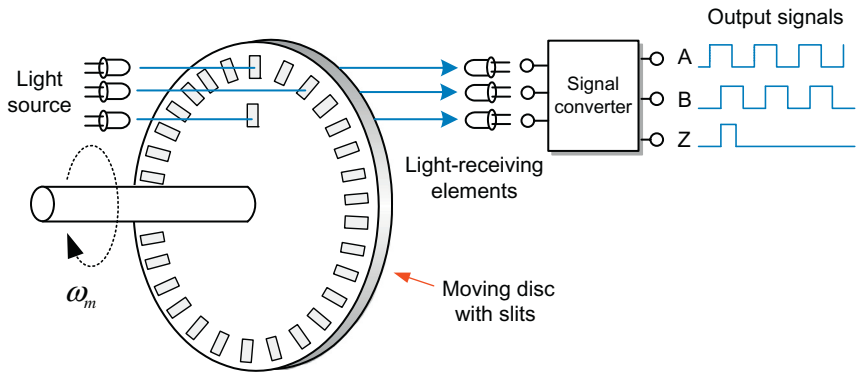

FIGURE 9.4

Simple configuration of an optical incremental encoder.

The encoders are a device that is sensitive to the surrounding environment such as temperature, shock, vibration, and contamination. To prevent noise from affecting encoder signals, it is preferable to use a shielded twisted pair cable for encoder output lines. Now we will explore how the incremental encoders work.

9.1.2.1 Operating principle of the optical incremental encoder

Fig. 9.4 shows the simple configuration of an optical incremental encoder, which consists of a moving disc mounted to the rotating shaft, light sources (LEDs), and light receivers (phototransistors). The moving disc has the same number of slits as PPR. The light of LEDs passing through the slits on the disc is transmitted to phototransistors, and in turn, is converted to square wave−shaped electric signals.

Commonly, the encoder has three outputs called A, B, and Z. The total number of A and B pulses per revolution is equal to PPR, with which the angular position and speed can be calculated. The A and B pulses are 90° out of phase, which allows the identification of the direction of rotation as shown in Fig. 9.5. For example, when rotating in the forward direction, pulse A is ahead of pulse B. There is another pulse Z known as the *index* or *reference pulse* besides pulses A and B. Pulse Z is generated once per revolution and can be used to set the reference position.

The absolute encoder is used when there is a need of an absolute position of the rotor. Since an absolute encoder generates a unique code (or multibit digital words) for each angular position of the rotor, we can find the actual position directly from the output signals. This output can be in binary code, binary coded decimal code, or gray code. The absolute encoder requires a complicated disc with many slits to generate the output code, resulting in a higher price.

Incremental encoders are the most widely used in motor drive applications. Since the incremental encoder produces a series of pulses as the rotor moves, we cannot measure the rotor speed directly from the encoders. Thus we will next discuss a method to estimate the speed from the output pulses of an encoder.

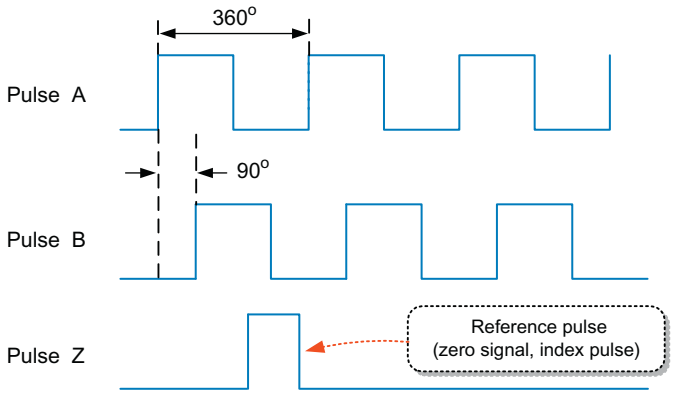

FIGURE 9.5

A, B, and Z pulses of incremental encoder.

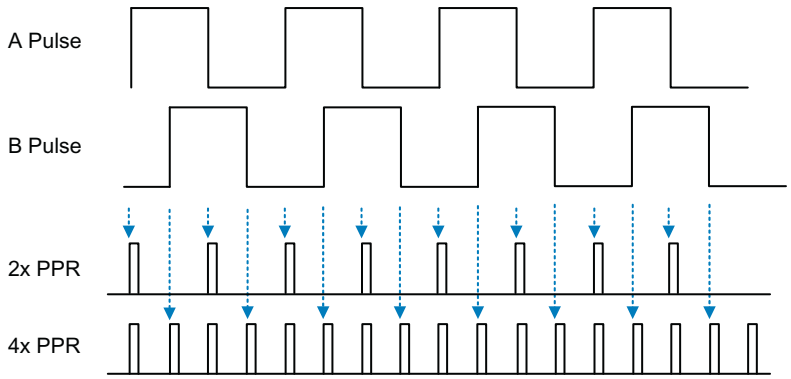

FIGURE 9.6

Pulse multiplication.

9.2 SPEED ESTIMATION USING AN INCREMENTAL ENCODER

We usually directly use the encoder pulses A or B themselves to calculate the speed. However, when more resolution is needed, we often increase the number of pulses by using a pulse multiplication. For a low-cost encoder with a low PPR, such multiplication can generate pulses more than the original pulse number, and thus results in a higher resolution. Fig. 9.6 shows that the PPR of an encoder can be doubled or quadrupled by counting the rising and falling edges of one or both pulses. In this way a 1000-PPR encoder can act like a 4000-PPR encoder by a 4× multiplication.

Now we will discuss how to calculate the speed of a rotor with pulses of an encoder mounted to the shaft of the rotor.

The angular velocity can be defined as the rate of change of the angular displacement X rad over the time interval T second as

$$\omega_m = \frac{X}{T} \quad (\text{rad/s}) \tag{9.2}$$

Here, the angular displacement X is obtained by counting the pulses produced from the encoder. The angular velocity can be often expressed in terms of revolution per minute unit as

$$N = \left(\frac{60}{2\pi}\right)\frac{X}{T} \quad (\text{r/min}) \tag{9.3}$$

There are three typical methods to obtain the angular velocity from the encoder pulses: M method, T method, and M/T method. In the M method, the angular velocity is obtained by measuring the displacement for a constant time interval. In the T method, the angular velocity is obtained by measuring the time interval for a constant displacement. Now, we will examine these methods in detail as follows.

9.2.1 M METHOD

In this method, the angular velocity is obtained by counting the pulses produced from the encoder during the constant sampling time interval T_c as shown in Fig. 9.7.

Assuming that the number of encoder pulses during the sampling time interval T_c is m, the angular displacement X over the T_c is given as

$$X = \frac{m}{PPR} \cdot 2\pi \quad (\text{rad}) \tag{9.4}$$

Thus the angular velocity is given from Eqs. (9.2) and (9.3) as

$$\omega_m = \frac{X}{T_c} = \frac{2\pi}{T_c}\frac{m}{PPR} \quad (\text{rad/s}) \tag{9.5}$$

$$N_f = \frac{60}{2\pi} \cdot \omega_m = \frac{60}{T_c} \cdot \frac{m}{PPR} \quad (\text{r/min}) \tag{9.6}$$

For example, if an encoder with a resolution of 1024 PPR produces 2048 pulses for 0.1 s, then the angular velocity can be calculated as

$$N = \frac{60 \cdot 2048}{0.1 \cdot 1024} = 1200 \text{ r/min} \tag{9.7}$$

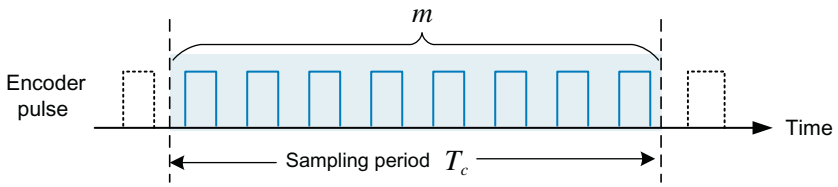

FIGURE 9.7

M method.

Since the M method is simple and easy to be implemented, it can be widely used in many applications where high precision in speed is not required. In addition, in this method, since the speed calculation time, i.e., the sampling time of the speed is constant, it is easy to design the speed controller where the speed is periodically controlled. The sampling period is commonly chosen within 1−3 ms according to the required control bandwidth. However, if the sampling time interval is not synchronous with pulses, as it is true in most cases, there exists a speed error. The maximum pulse error is one pulse, resulting in a maximum speed error of $60/(T_c \text{ PPR})$ (r/min). For example, for PPR = 2000, 4× multiplication, and $T_c = 1$ ms, the maximum speed error is $(60/(1 \text{ ms} \times 4 \times 2000)) = 7.5$ r/min. Thus in this case, it is impossible to identify a speed less than 7.5 r/min. In particular, this absolute pulse error of one pulse deteriorates the accuracy of the calculated speed in the low-speed region. It is because, in the low-speed region, the number of pulses becomes low as shown in Fig. 9.8. Thus this method is more effective in the high-speed region where there is are a large number of pulses. To reduce the speed error, it is necessary to use a large PPR or a long sampling time interval. However, a long time interval reduces the speed control bandwidth as we discussed in Chapter 2. Thus it is desirable to use an encoder with a large PPR, but it is an expensive solution.

9.2.2 T METHOD

In this method, the angular velocity is obtained by measuring the time interval T_c between two consecutive pulses to eliminate the pulse error as shown in Fig. 9.9.

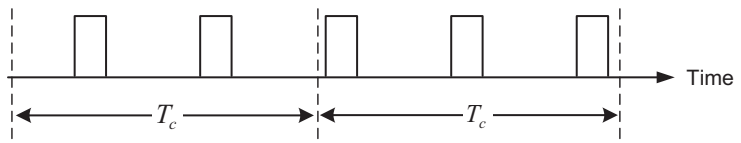

FIGURE 9.8

Pulse error in the low-speed region.

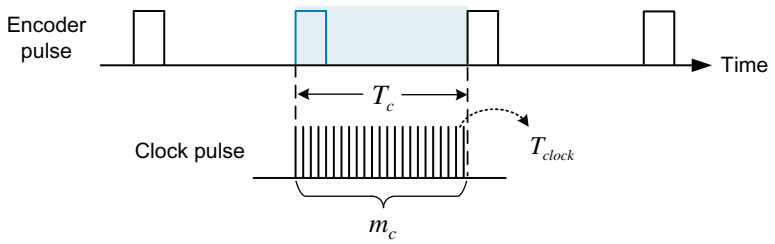

FIGURE 9.9

T method.

In the T method, the angular displacement X is always fixed as

$$X = \frac{2\pi}{PPR} \quad \text{(rad)} \tag{9.8}$$

The time interval T_c between two pulses is estimated by counting a reference clock, whose frequency is high enough compared to that of the encoder pulse. Assuming that the period of the reference clock is T_{clock} and the number of the reference clock generated for the time between two pulses is m_c, then the time T_c is given as

$$T_c = m_c \cdot T_{clock} \quad \text{(s)} \tag{9.9}$$

Thus the angular velocity is given as

$$\omega_m = \frac{X}{T} = \frac{2\pi}{PPR} \cdot \frac{1}{m_c T_{clock}} \quad \text{(rad/s)} \tag{9.10}$$

$$N = \frac{60}{2\pi} \cdot \omega_m = \frac{60}{PPR} \cdot \frac{60}{m_c \cdot T_{clock}} \quad \text{(r/min)} \tag{9.11}$$

Unlike the M method, the T method has an advantage of enabling an accurate calculation in the low-speed region because it has no pulse omitting. On the other hand, in the high-speed region, the frequency of the reference clock should be high enough to calculate the pulse period accurately. However, when such high-frequency reference clock is used, a clock counter with large bits is required for the operation in the low-speed region. Besides these, the calculation of Eq. (9.11) requires a division, which takes a long calculation time for a digital controller. Moreover, since the speed calculation time T_c varies with the speed, this method is not preferable for use for a speed controller, which carries out the speed control at each constant time interval.

9.2.3 M/T METHOD

The M/T method combines the two methods explained previously, which improves the accuracy of the speed calculation. The M/T method is now widely used in many motor drive applications for obtaining the speed information with a high resolution.

In the M/T method, similar to the M method, the encoder pulses are first counted in the constant sampling time interval T_c. However, if the sampling time does not synchronize with the last pulse, the extra time ΔT to the last pulse is additionally measured to eliminate the pulse error by adopting the T method as shown in Fig. 9.10. Thus in this method, the angular velocity can be calculated accurately by measuring the total time $T(= T_c + \Delta T)$ for the encoder pulses m_1.

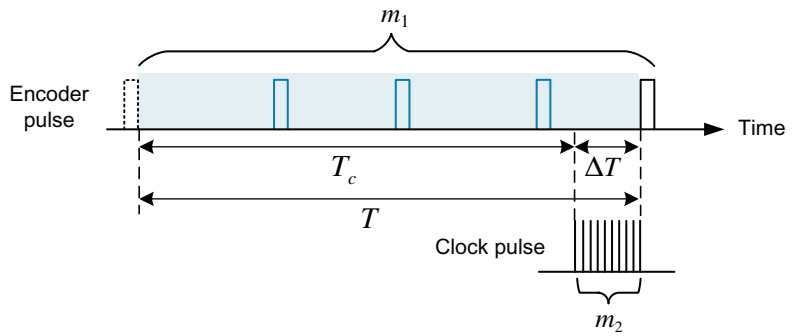

FIGURE 9.10

M/T method.

For the number of the encoder pulses m_1, the angular displacement X is given as

$$X = \frac{2\pi}{PPR} m_1 \quad \text{(rad)} \tag{9.12}$$

If the period of the reference clock is T_2 and counts of the number of the clock pulses is m_2, the total duration time for the pulses m_1 is given as

$$T = T_c + \Delta T = T_c + T_2 m_2 \quad \text{(s)} \tag{9.13}$$

Then the angular velocity is given as

$$\omega_m = \frac{X}{T} = \frac{2\pi}{PPR} \cdot \frac{m_1}{T_c + m_2 T_2} \quad \text{(rad/s)} \tag{9.14}$$

$$N = \frac{60}{2\pi} \cdot \omega_m = \frac{60}{PPR} \cdot \frac{m_1}{T_c + m_2 T_2} \quad \text{(r/min)} \tag{9.15}$$

The speed calculation based on the M/T method is more accurate than the other two methods, but its implementation is quite difficult. The M/T method has a problem in the very low-speed region. Since, in the very low-speed region, the number of the encoder pulses is too small, the extra time ΔT may be larger than the sampling time interval T_c. Thus the period for the speed calculation can vary with the speed.

The speed estimation methods introduced above cannot inherently estimate the true instantaneous speed, but only a discrete average speed over the sample interval. Since the actual speed within the sampling period interval cannot be identified, the speed control cannot work properly for a system with a long sampling period. In addition, a system with a high bandwidth of speed control may become unstable in the low-speed region, where the speed detection delay time is long. To overcome this problem, we need to estimate the instantaneous speed by using a *position observer* or a *state filter* with the discrete average speed obtained from the encoder pulses [4,5].

9.3 SENSORLESS CONTROL OF ALTERNATING CURRENT MOTORS

The vector control of AC motors requires the position of the rotor flux. The knowledge of the rotor position is used for identifying the position of the rotor flux. For this purpose, a position sensor such as an encoder or a resolver is installed at the rotor shaft as shown in Fig. 9.11.

A resolver is usually used for PMSM drives that require an absolute position of the rotor for start-up and vector control. On the other hand, an incremental encoder to measure the angular displacement of the rotor is commonly used for induction motor drives. When an incremental encoder is used for PMSMs, the initial rotor position should be provided [6].

Such position sensors cause several problems. Above all, these sensors increase the cost of the whole motor drive system. These sensors are also sensitive to the surrounding environment. The DC power lines and interface lines for a sensor increase the complexity of the system and are susceptible to noise. This may degrade the system reliability. In addition, the sensor attached to the shaft of a motor increases its size and requires maintenance periodically.

To solve this problem, a control technology without any position sensor, referred as *sensorless control*, has emerged and become an important research subject in the field of AC motor drives. The vector control using a sensor can

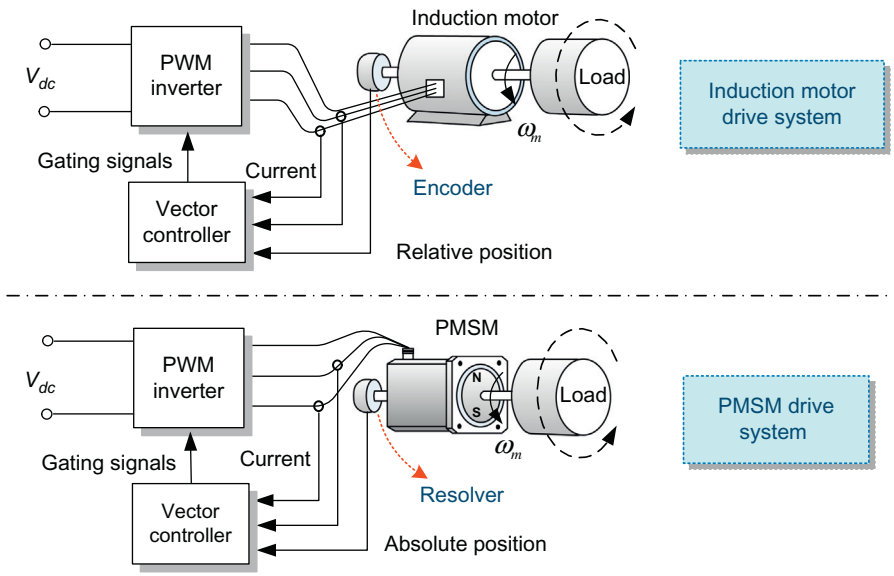

FIGURE 9.11

Position sensor for AC motor drive systems.

provide the speed accuracy of $\pm 0.01\%$ and the speed control range of 1:1000. These days, the sensorless vector control can provide a speed accuracy of $\pm 0.5\%$ and a speed control range of 1:150. The performance of the sensorless vector control exceeds that of the scalar control such as the *V/f* control, which has a speed accuracy of $\pm 1 \sim 2\%$. Nowadays, sensorless control techniques to achieve a performance comparable to that of the sensored vector control have been investigated continuously.

Understanding the sensorless control techniques requires a comprehensive knowledge of the motor control that was stated in the previous chapters 4–8. Now we will review briefly the sensorless control techniques of AC motors.

9.3.1 TYPES OF SENSORLESS CONTROL

For more than two decades, many efforts have been made to develop a sensorless drive of AC motors. These sensorless techniques are subdivided into two major groups according to their method of deriving the rotor position as shown in Fig. 9.12. One typical group is based on back-electromotive force (EMF) retaining information on the rotor speed [7–17]. The technique of this group is that the rotor position can be obtained through an estimator or observer using mathematical equations of a motor. Another group obtains the rotor position from the characteristics of a motor itself [18–24]. In this technique, a special signal to extract the rotor position-dependent characteristics from a motor is injected into the motor. High-frequency voltage is commonly used as the special signal.

9.3.1.1 Sensorless technique using the motor model

The basic concept of this sensorless technique is to use the back-EMF retaining information on the rotor speed to obtain the rotor flux position [7–17]. This sensorless technique usually uses an estimator or observer to obtain the rotor flux

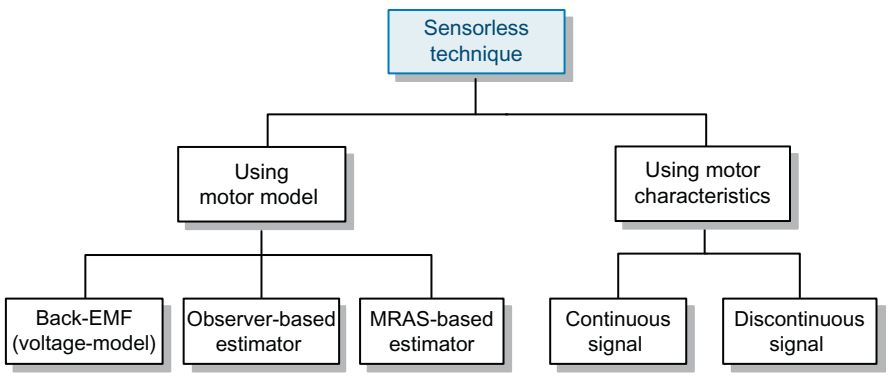

FIGURE 9.12

Different types of sensorless control methods.

position or the rotor flux linkage by using mathematical equations of a motor with its measured voltage and current.

We have already seen one example of the sensorless control of an induction motor based on this concept in Chapter 5. In the voltage model of Section 5.3.1, it was seen that the rotor flux angle could be estimated from the rotor flux linkage obtained by using the stator voltage equations. We will now review this process. The stator flux linkages are obtained first by the integral of back-EMFs, and in turn, the rotor flux linkages are estimated from the stator flux linkages as

$$\hat{\lambda}^s_{dqs} = \int (v^s_{dqs} - R_s i^s_{dqs})dt = \int e^s_{dqs}dt \rightarrow \hat{\lambda}^s_{dqr} = \frac{L_r}{L_m}(\hat{\lambda}^s_{dqs} - \sigma L_s i^s_{dqs}) \tag{9.16}$$

From the rotor flux linkages, the rotor flux angle $\hat{\theta}_e$ and the rotor speed $\hat{\omega}_r$ can be estimated as

$$\hat{\theta}_e = \tan^{-1}\left(\frac{\hat{\lambda}^s_{qr}}{\hat{\lambda}^s_{dr}}\right) \tag{9.17}$$

$$\hat{\omega}_e = \frac{d\hat{\theta}_e}{dt} = \frac{d}{dt}\left[\tan^{-1}\left(\frac{\hat{\lambda}^s_{qr}}{\hat{\lambda}^s_{dr}}\right)\right] \tag{9.18}$$

$$\hat{\omega}_r = \hat{\omega}_e - \omega_{sl} \tag{9.19}$$

Likewise, for a PMSM, the rotor flux angle $\hat{\theta}_r$ and the rotor speed $\hat{\omega}_r$ can be estimated by using the stator voltage and the stator flux linkage equations as

$$\begin{aligned}\hat{\lambda}^s_{dqs} &= \int (v^s_{dqs} - R_s i^s_{dqs})dt \\ &= \int e^s_{dqs}dt \quad (e^s_{dqs} = v^s_{dqs} - R_s i^s_{dqs})\end{aligned} \tag{9.20}$$

$$\hat{\theta}_r = \tan^{-1}\left(\frac{\hat{\lambda}^s_{qr}}{\hat{\lambda}^s_{dr}}\right) = \tan^{-1}\left(\frac{\hat{\lambda}^s_{qs} - L_s i^s_{qs}}{\hat{\lambda}^s_{ds} - L_s i^s_{ds}}\right) \tag{9.21}$$

$$\hat{\omega}_r = \frac{d\hat{\theta}_r}{dt} \tag{9.22}$$

As we can see, the sensorless control technique based on the motor model is simple compared to the other methods using the characteristics of a motor and is capable of providing a satisfactory estimating performance in the medium- to high-speed range. However, since it is based on the back-EMF proportional to a rotor speed, its performance is inevitably limited in the low-speed range. A satisfactory performance cannot be obtained 10% below the rated speed. Especially, at zero speed where the back-EMF is equal to zero (or at zero stator frequency for an induction motor), no information on the rotor flux can be acquired, so this technique will fail to control the motor. Therefore this sensorless control technique is not an easy task to improve the performance in the low-speed range and at zero speed.

The accuracy of the estimation obtained from the sensorless control technique based on the motor model depends on the accuracy of motor parameters and input values used in the model as well as the accuracy of the model itself. The motor parameters can vary easily according to operating conditions such as winding temperature and flux level. The variation of parameters has influence on the accuracy of the estimation. For example, it can be readily seen that an accurate information on the stator resistance is required to estimate the stator flux linkage accurately from Eq. (9.16) or (9.20). Thus for an accurate sensorless control, an algorithm which provides real-time adaptation for motor parameters is necessary. The input values used in the model such as the current and voltage of the motor should also be measured precisely. Mostly, the motor currents are directly measured by using current sensors. However, since the voltages applied to the motor are generated as a pulse width modulation (PWM) waveform, it is hard to be directly measured. Thus voltage commands or output voltages calculated reversely by the switching pattern of an inverter are commonly used instead. In this case, as stated in Chapter 7, nonlinearity of an inverter due to a voltage drop on the switching devices and the dead time effect should be considered.

As a type of this sensorless control method for induction motors, the model reference adaptive control (MRAC) method, which estimates the rotor speed by comparing outputs of two models that estimate the rotor flux linkage, is a classic example [7,8]. Besides the MRAC, several techniques using the advanced control theory, such as the adaptive speed observer or Kalman filter, have been developed [9,10]. The stable operation region for such sensorless control methods is limited to 1−3 Hz due to insufficient back-EMF information in the low-speed range. However, some researches to further lower the available operating range have been proposed [11].

Several approaches used for induction motors are also adopted for the sensorless control of PMSMs such as a method estimating the rotor position from the flux obtained by an integral of back-EMF [13], a method adopting the MRAC using the error between outputs of two motor models [13,14], and a method using the advanced control theory such as the state observer or Kalman filter [15−17].

9.3.1.2 Sensorless technique using the characteristics of a motor

Sensorless control methods using the motor model mentioned previously cannot inherently avoid performance degradation in the low-speed range and at zero speed due to their dependency on back-EMF. Thus sensorless control methods using a different concept have been researched. These methods derive information on the rotor position from secondary effects of a motor such as eccentricity of a rotor, magnetic saliency, and slot harmonics [18,19]. Since these characteristics appear regardless of the rotor speed, they can be exploited for sensorless control even in the low-speed range and at zero speed.

Most of these sensorless methods exploit spatial magnetic saliency, which indicates the spatial variation of the inductance according to the rotor position

[20–25]. In this case, a special signal is injected into the motor to extract the magnetic saliency. A discontinuous pulse signal or modified PWM signal can be used as the injected signal, but a continuous high-frequency signal of a sinusoidal waveform is mainly used. Voltage rather than current has been mainly used as a type of high-frequency injection signal. The high-frequency injection voltage is added to the output of the current controller. The rotor position can be estimated from the motor's response to the injected voltage signal because the motor's response varies according to the magnetic saliency. The high-frequency signal enables us to estimate the magnetic saliency for a surface-mounted permanent magnet synchronous motor or an induction motor without magnetic saliency on its rotor as well as an interior permanent magnet synchronous motor with magnetic saliency on its rotor.

Fig. 9.13 shows a block diagram of a typical sensorless drive based on the high-frequency signal injection. The sensorless drive system consists of three parts. First one is a high-frequency signal injection part, which injects a special signal continuously to obtain the saliency information of the motor. Another is a signal processing part, which decomposes the current induced by the injected voltage and extracts the rotor position-related value. Finally, there is a position observer part, which estimates the rotor position and speed from the extracted rotor position-related value.

In the high-frequency signal injection, it is known that the voltage signal injection into the *d*-axis of the estimated rotor reference frame can result in a simpler signal processing and a better performance, even though the signal can be injected into any reference frame. The signal processing part often requires low-pass filters to extract the fundamental current and band-pass filters to extract the injected frequency component current from the measured motor current. Time delay by these filters limits the control bandwidth of the sensorless drives. The bandwidth of the speed controller is usually only about several Hertz.

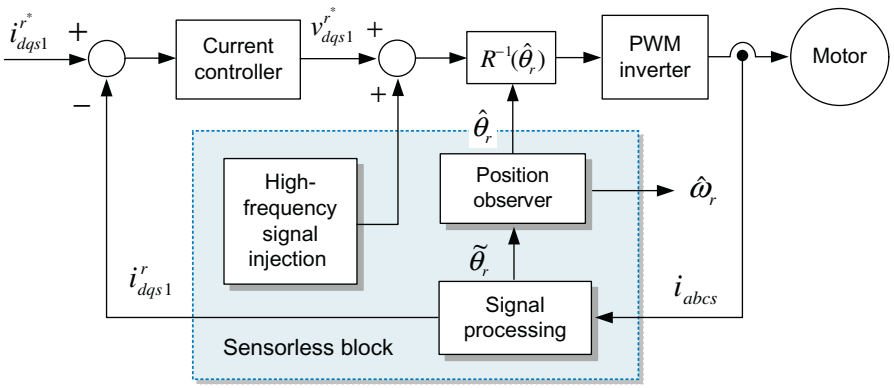

FIGURE 9.13

Typical sensorless drive system based on the high-frequency signal injection.

Recently, instead of the conventional sinusoidal-type signal injection, a square wave−type voltage injection has been proposed to eliminate the low-pass filters for the signal processing and enhance the control bandwidth of the sensorless drives. In these methods, the control bandwidth is very close to the value available in sensored drives [22−24].

The sensorless control methods using magnetic saliency and high-frequency voltage injection give a complex signal processing to estimate the rotor position information, requiring a high-performance microprocessor. In addition, the voltage injected to extract the rotor position produces an additional loss, acoustic noise, and torque ripple. Another problem is that there is a voltage shortage in the high-speed operation because an extra voltage is used to generate the injection signal. Thus this leads to a loss of high-speed operation. To overcome this problem, hybrid sensorless methods combing the two techniques mentioned above have been proposed for operation in the entire speed range [25]. The hybrid sensorless methods use the high-frequency signal injection technique at low-speed region and at zero speed but the back-EMF technique at a higher speed region, in which sufficient back-EMF information is available. In the hybrid methods, a transition between the two techniques is an important issue.

REFERENCES

[1] <http://www.amci.com/tutorials/tutorials-what-is-resolver.asp>.

[2] D.C. Hanselman, Resolver signal requirement for high accuracy resolver-to-digital conversion, IEEE Trans. Ind. Electron. 37 (6) (Dec. 1990) 556−561.

[3] H.-S. Mok, S.-H. Kim, Y.-H. Cho, Torque ripple reduction of PMSM caused by position sensor error for EPS application, Electron. Lett. 43 (11) (2007) 646−647.

[4] H.W. Kim, S.K. Sul, A new motor speed estimator using Kalman filter in low-speed range, IEEE Trans. Ind. Electron. 43 (4) (Aug. 1996) 498−504.

[5] R.D. Lorenz, K.V. Patten, High-resolution velocity estimation for all-digital AC servo drives, IEEE Trans. Ind. Appl. 27 (4) (Aug. 1991) 701−705.

[6] N.-C. Park, Y.-K. Lee, S.-H. Kim, Initial rotor position estimation for an interior permanent-magnet synchronous motor using inductance saturation, Trans. Korean Inst. Power Electron. 16 (4) (Aug. 2011) 374−381.

[7] C. Schauder, Adaptive speed identification for vector control of induction motors without rotational transducers, IEEE Trans. Ind. Appl. 28 (5) (Sep./Oct. 1992) 1054−1061.

[8] T. Ohtani, N. Takada, K. Tanaka, Vector control of induction motor without shaft encoder, IEEE Trans. Ind. Appl. 28 (1) (Jan./Feb., 1992) 157−164.

[9] H. Kubota, K. Matsuse, T. Nakano, DSP-based adaptive flux observer of induction motor, IEEE Trans. Ind. Appl. 29 (2) (Mar./Apr. 1993) 344−348.

[10] Y.R. Kim, S.K. Sul, M.H. Park, Speed sensorless vector control of induction motor using extended Kalman filter, IEEE Trans. Ind. Appl. 30 (5) (Sep./Oct. 1994) 1225−1233.

[11] J. Holtz, Sensorless control of induction motor drives, Proc. IEEE 90 (8) (Aug. 2002) 1359−1394.

[12] R. Wu, G.R. Slemon, A permanent magnet motor drive without a shaft sensor, IEEE Trans. Ind. Appl. 27 (5) (Sep./Oct. 1991) 1005–1011.
[13] N. Matsui, M. Shigyo, Brushless DC motor control without position and speed sensor, IEEE Trans. Ind. Appl. 28 (1) (1992) 120–127.
[14] N. Matsui, T. Takeshita, K. Yasuda, A new sensorless drive of brushless DC motor, in: Proc. 1992 Int. Conf. IECON, 1992, pp. 430–435.
[15] L.A. Jones, J.H. Lang, A state observer for the permanent-magnet synchronous motor, IEEE Trans. Ind. Electron. 36 (3) (1989) 374–382.
[16] Z. Chen, M. Tomita, S. Doki, S. Okuma, An extended electromotive force model for sensorless control of interior permanent magnet synchronous motors, IEEE Trans. Ind. Appl. 38 (2) (2003) 288–295.
[17] S. Bolognani, R. Oboe, M. Zigliotto, Sensorless full-digital PMSM drive with EMF estimation of speed and rotor position, IEEE Trans. Ind. Electron. 46 (2) (1999) 240–247.
[18] R. Blasco-Gimenez, G.M. Asher, M. Sumner, K.J. Bradley, Performance of FFT-rotor slot harmonic speed detector for sensorless induction motor drives, IEE Proc. Elect. Power Appl. 143 (3) (May 1996) 258–268.
[19] M. Schroedl, Sensorless control of AC machines at low speed and standstill based on "INFORM" method, in: Conf. Rec. IEEE IAS Annu. Meeting, 1996, pp. 270–277.
[20] J.-I. Ha, S.-K. Sul, Sensorless field-orientation control of an induction, IEEE Trans. Ind. Appl. 35 (1) (Jan./Feb. 1999) 45–51.
[21] J. Holtz, Sensorless control of induction machines-with or without signal injection?, IEEE Trans. Ind. Electron. 53 (1) (2006) 7–30.
[22] Y.-D. Yoon, S.-K. Sul, S. Morimoto, K. Ide, High-bandwidth sensorless algorithm for AC machines based on square-wave-type voltage injection, IEEE Trans. Ind. Appl. 47 (3) (2011) 1361–1370.
[23] S.-M. Kim, J.-I. Ha, S.-K. Sul, PWM switching frequency signal injection sensorless method in IPMSM, IEEE Trans. Ind. Appl. 48 (5) (2012) 1576–1586.
[24] N. Park, S.-H. Kim, A simple sensorless algorithm for IPMSMs based on high-frequency voltage injection method, IET Elect. Power Appl. 8 (2) (2014) 68–75.
[25] K. Ide, J.-I. Ha, M. Sawamura, A hybrid speed estimator of flux observer for induction motor drives, IEEE Trans. Ind. Electron. 53 (1) (2006) 130–137.